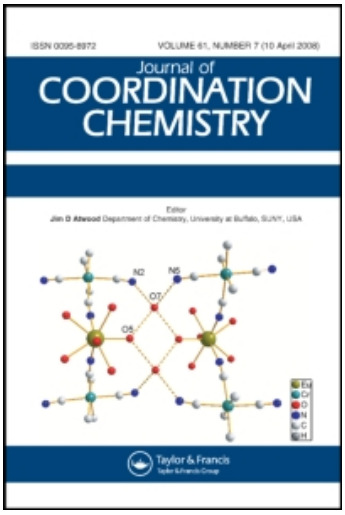

Journal of Coordination Chemistry
Publication details, including instructions for authors and subscription information:
http://www.informaworld.com/smpp/title~content=t713455674

DNA interaction studies of ruthenium(II) polypyridyl complex : $[Ru(dmb)_2(ITAP)](ClO_4)_2$ (ITAP = isatino [1,2-b]-1,4,8,9-tetraazatriphenylene)

Fu-Hai Wu[a]; Cheng-Hui Zeng[b]; Yun-Jun Liu[b]; Xiao-Yan Guan[b]; Li-Xin He[b]
[a] School of Public Health, Guangdong Pharmaceutical University, Guangzhou, P.R. China [b] School of Pharmacy, Guangdong Pharmaceutical University, Guangzhou, P.R. China

First published on: 22 September 2010

To cite this Article Wu, Fu-Hai , Zeng, Cheng-Hui , Liu, Yun-Jun , Guan, Xiao-Yan and He, Li-Xin(2009) 'DNA interaction studies of ruthenium(II) polypyridyl complex : $[Ru(dmb)_2(ITAP)](ClO_4)_2$ (ITAP = isatino [1,2-b]-1,4,8,9-tetraazatriphenylene)', Journal of Coordination Chemistry, 62: 21, 3512 — 3521, First published on: 22 September 2010 (iFirst)
To link to this Article: DOI: 10.1080/00958970903095806
URL: http://dx.doi.org/10.1080/00958970903095806

Journal of Coordination Chemistry
Vol. 62, No. 21, 10 November 2009, 3512–3521

DNA interaction studies of ruthenium(II) polypyridyl complex : $[Ru(dmb)_2(ITAP)](ClO_4)_2$ (ITAP = isatino [1,2-b]-1,4,8,9-tetraazatriphenylene)

FU-HAI WU†, CHENG-HUI ZENG‡, YUN-JUN LIU*‡, XIAO-YAN GUAN‡ and LI-XIN HE‡

†School of Public Health, Guangdong Pharmaceutical University, Guangzhou 510006, P.R. China
‡School of Pharmacy, Guangdong Pharmaceutical University, Guangzhou 510006, P.R. China

(*Received 16 October 2008; in final form 18 March 2009*)

A new ligand ITAP and its complex $[Ru(dmb)_2(ITAP)](ClO_4)_2$ (ITAP = isatino [1,2-b]-1,4,8,9-tetraazatriphenylene, dmb = 4,4′-dimethyl-2,2′-bipyridine) have been synthesized and characterized by elemental analysis, Fast atom bombardment mass spectra, Electrospray mass spectra, and ^1H NMR. Thermal denaturation and absorption titration experiments show the complex binds to calf thymus DNA (CT-DNA) with moderate affinities. Viscosity measurements and thermal denaturation indicate that the DNA-binding mode could be intercalative interaction. The Ru(II) complex in the presence of plasmid pBR322 DNA has been found to promote the cleavage of plasmid pBR322 DNA from the supercoiled Form I to the open circular Form II upon irradiation. Mechanisms for DNA cleavage by the complex were also investigated.

Keywords: Ruthenium(II) complex; DNA-binding; Photo-induced cleavage

1. Introduction

Studies on the interaction of transition metal complexes with nucleic acids have gained prominence because of their relevance in the development of new reagents for biotechnology and medicine. These studies are also important for the development of probes of nucleic acid structure [1–4]. $[Ru(bpy)_2(dppz)]^{2+}$ (bpy = 2,2′-bipyridine) and $[Ru(phen)_2(dppz)]^{2+}$ (phen = 1,10-phenanthroline, dppz = dipyrido [3,2-*a*:2′,3′-*c*] phenazine) show no luminescence in aqueous solution at ambient temperature, but luminesce was brightly upon binding intercalatively with the dppz ligand between adjacent DNA base pairs, characteristic of ''molecule light switches'' [5–8]. The luminescence enhancement was proposed to be the protection of phenanzine

*Corresponding author. Email: lyjche@163.com

ISSN 0095-8972 print/ISSN 1029-0389 online © 2009 Taylor & Francis
DOI: 10.1080/00958970903095806

nitrogen from water when the dppz ligand intercalated between base pairs of DNA. These complexes bind to DNA through three types of weak interactions: (i) electrostatic binding, involving interactions between the cationic metal complex, and the negatively charged phosphates of DNA; (ii) ligand π-stacking interactions, characterized by intercalation of an extended planar aromatic ring system (two or three six-membered rings), between base pairs, through the major or minor grooves of the nucleic acid helix; and (iii) groove binding, associated by hydrogen bonds, and/or van der Waals interactions along the groove of the duplex. In contrast to the intercalation mode, groove binding does not significantly perturb the DNA structure [9, 10]. To obtain effective DNA cleavage reagents, photo-induced cleavage of supercoiled plasmid DNA (pBR322 DNA) is important; photo-induced cleavage of DNA by a variety of metal complexes, predominantly ruthenium complexes [11–14] and metalloporphyrins [15, 16], has been reported. Swavey and Brewer [17] reported that $[\{(bpy)_2Ru(dpp)\}_2RhCl_2]$ (dpp = 2,3-*bis*(2-pyridyl)pyrazine) induces photocleavage of DNA in visible light, the first supermolecular system shown to cleave DNA. We have been interested in synthesizing new polypyridyl ruthenium(II) complexes and studying their interactions with DNA to elucidate DNA-binding and photo-induced cleavage mechanism. In this aricle, ITAP and its complex $[Ru(dmb)_2(ITAP)](ClO_4)_2$ (dmb = 4,4′-dimethyl-2, 2′-bipyridine, ITAP = isatino [1,2-b]-1,4,8,9-tetraazatriphenylene, Supplemental material) were synthesized and characterized by elemental analysis, Fast atom bombardment mass spectra (FAB-MS), Electrospray mass spectra (ESI-MS), and ^{1}H NMR. The interactions of the complex with calf thymus DNA (CT-DNA) were investigated by electronic absorption, viscosity measurement, thermal denaturation, and photo-induced cleavage. The complex has moderate affinity to DNA. Mechanistic studies of photocleavage reveal that singlet oxygen ($^1O_2$) and superoxide anion radical ($O_2^{\bullet-}$) may play an important role in photocleavage. The DNA-binding affinity for $[Ru(dmb)_2(ITAP)]^{2+}$ is smaller than that of $[Ru(bpy)_2(dppz)]^{2+}$ [18], owing to the greater planarity of dppz compared with ITAP.

2. Experimental

2.1. *Material and methods*

All reagents and solvents were purchased commercially and used without purification unless otherwise noted. Doubly distilled water was used to prepare buffer (5 mM *tris*(hydroxymethylaminomethane)-HCl, 50 mM NaCl, pH = 7.2). CT-DNA was obtained from the Sino-American Biotechnology Company. A solution of CT-DNA in the buffer gave a ratio of UV absorbance at 260 and 280 nm of 1.8–1.9 : 1, indicating the DNA was sufficiently free of protein. [19]. The DNA concentration per nucleotide was determined by absorption spectroscopy using the molar absorption coefficient (6600 $M^{-1}\,cm^{-1}$) at 260 nm [20].

2.2. *Synthesis of ligand and complex*

2.2.1. Isatino [1,2-b]-1,4,8,9-tetraazatriphenylene (ITAP). A mixture of 5,6-diamino-1,10-phenanthroline (0.21 g, 1.0 mmol) [21, 22], isatin (0.15 g, 1.0 mmol), and glacial

acetic acid (20 cm^3) was refluxed under argon for 6 h, then cooled to room temperature and diluted with water (*ca* 50 cm^3). Dropwise addition of concentrated aqueous ammonia to neutralize gave a yellow-green precipitate, which was collected and washed with water and small amounts of cool ethanol. The crude product dissolved in ethanol was purified by filtration on silica gel (100–200 mesh). The principal band was collected and then evaporation of the solution gave yellow-green powder which was dried at 50°C *in vacuo*. Yield: 70%. Found (%): C, 74.78; H, 3.43; N, 21.83. Calcd for $C_{20}H_{11}N_5$ (%): C, 74.76; H, 3.45; N, 21.79%. ^{1}H NMR (ppm, DMSO-d_6): δ 11.56 (s, 1H), 10.04 (d, 1H, $J = 8.8$ Hz), 9.15 (d, 1H, $J = 8.7$ Hz), 8.89 (d, 1H, $J = 8.7$ Hz), 8.82 (d, 1H, $J = 8.6$ Hz), 8.48 (d, 1H, $J = 8.8$ Hz), 7.42–7.49 (m, 2H), 7.25 (d, 1H, $J = 8.5$ Hz), 7.09–7.17 (m, 2H). FAB-MS: $m/z = 322$ ($[M + 1]^+$).

2.2.2. [Ru(dmb)$_2$(ITAP)](ClO$_4$)$_2$. A mixture of *cis*-$[Ru(dmb)_2Cl_2] \cdot 2H_2O$ (0.288 g, 0.5 mmol) [23] and ITAP (0.161 g, 0.5 mmol) in EtOH (40 cm^3) was refluxed under argon for 8 h to give a clear red solution. Upon cooling, a red precipitate was obtained by dropwise addition of saturated aqueous $NaClO_4$ solution. The crude product was purified by column chromatography on neutral alumina with CH_3CN : toluene (3 : 1, v/v) as eluent. The brown red band was collected. The solvent was removed under reduced pressure giving a red powder. Yield: 64%. Found (%): C, 53.41; H, 3.55; N, 12.72. Calcd. for $C_{44}H_{35}N_9Cl_2O_8Ru$ (%): C, 53.39; H, 3.56; N, 12.74%. ^{1}H NMR (ppm, DMSO-d_6): δ 12.89 (s, 1H, N–H), 9.70 (d, 1H, H_a, $J = 8.6$ Hz), 9.55 (d, 1H, $H_{a'}$, $J = 8.4$ Hz), 8.75 (d, 4H, H_2, $H_{2'}$, $J = 8.8$ Hz), 8.54 (d, 2H, H_c, $H_{c'}$, $J = 8.4$ Hz), 8.30 (s, 4H, H_5, $H_{5'}$), 8.24 (d, 1H, H_d, $J = 8.0$ Hz), 8.20 (d, 1H, H_g, $J = 8.0$ Hz), 8.00–8.05 (m, 2H, H_b, $H_{b'}$), 7.91 (t, 2H, H_3, $J = 7.5$ Hz), 7.82 (t, 2H, $H_{3'}$, $J = 7.82$ Hz), 7.50–7.56 (m, 1H, H_f), 7.40–7.45 (m, 1H, H_e), 3.30 (s, 6H), 3.26 (s, 6H). ESI-MS (CH_3CN): m/z 890.4 ($[M - ClO_4]^+$), 395.3 ($[M - 2ClO_4]^{2+}$).

Caution: Perchlorate salts of metal complexes with organic ligands are potentially explosive, and only small amounts of the material should be prepared and handled with great care.

2.3. *Physical measurements*

Microanalysis (C, H, and N) was carried out with a Perkin-Elmer 240Q elemental analyzer FAB-MS were recorded on a VG ZAB-HS spectrometer in a 3-nitrobenzyl alcohol matrix. ESI-MS were recorded on a LCQ system (Finnigan MAT, USA) using methanol as mobile phase. The spray voltage, tube lens offset, capillary voltage, and capillary temperature were set at 4.50 KV, 30.00 V, 23.00 V and 200°C, respectively, and the quoted m/z values are for the major peaks in the isotope distribution. ^{1}H NMR spectra were recorded on a Varian-500 spectrometer. All chemical shifts were given relative to tetramethylsilane (TMS). UV-Vis spectra were recorded on a Shimadzu UV-3101PC spectrophotometer at room temperature. Cyclic voltammetric measurements were performed on a CHI 660A Electrochemical Workstation. All samples were purged with nitrogen prior to measurements. A standard three-electrode system of platinum microcylinder working electrode, platinum-wire auxiliary electrode and a saturated calomel reference electrode (SCE) was used.

2.4. *DNA-binding and photo-induced cleavage*

Absorption titrations of ruthenium(II) complexes in buffer were performed by using a fixed ruthenium concentration to which increments of the DNA stock solution were added. Ruthenium-solutions employed are 20 μM and CT-DNA was added to a ratio of 7.2 : 1 of [DNA] : [Ru]. Ruthenium–DNA solutions were allowed to incubate for 5 min before the absorption spectra were recorded. The intrinsic binding constants K_b of Ru(II) complexes to DNA were derived from equation (1) [24–26].

$$\frac{\varepsilon_a - \varepsilon_f}{\varepsilon_b - \varepsilon_f} = \frac{\sqrt{(b - (b^2 - 2K^2C_t[\mathrm{DNA}]/s)}}{2KC_t} \quad (1)$$

$$b = 1 + KC_t + K[\mathrm{DNA}]/2s \quad (2)$$

where [DNA] is the concentration of CT-DNA in base pairs, the apparent absorption coefficients ε_a, ε_f, and ε_b correspond to A_{obsd}/[Ru], the absorbance for the free ruthenium complex and the absorbance for the ruthenium complex in fully bound form, respectively. K is the equilibrium binding constant, C_t is the total metal complex concentration in nucleotides, and s is the binding site size.

Thermal denaturation studies were carried out with a Perkin–Elmer Lambda 35 spectrophotometer equipped with a Peltier temperature-controlling programmer (±0.1°C). The temperature of the cell containing the cuvette was ramped from 50 to 90°C, and the absorbance at 260 nm was continuously monitored for the solutions of CT-DNA (80 μM) in the absence and presence of complex. The temperature of the solution was increased by 1°C min^{-1}.

Viscosity measurements were carried out using an Ubbelodhe viscometer maintained at 28.0 (±0.1)°C in a thermostatic bath. DNA samples approximately 200 base pairs in average length were prepared by sonicating in order to minimize the complexities arising from DNA flexibility [27]. Flow time was measured with a digital stopwatch, each sample was measured three times, and an average flow time was calculated. Data are presented as $(\eta/\eta_0)^{1/3}$ *versus* binding ratio [28], where η is the viscosity of DNA in the presence of complex and η_0 is the viscosity of DNA alone.

For the gel electrophoresis experiment, supercoiled pBR322 DNA (0.1 μg) was treated with the Ru(II) complex in 50 mM Tris-acetate, 18 mM NaCl buffer, and the solution was then irradiated at room temperature with a UV lamp (365 nm, 10 W). Samples were analyzed by eletrophoresis for 1 h at 100 V on a 0.8% agarose gel in Tris-acetate buffer. The gel was stained with 1 μg mL^{-1} ethidium bromide (EB) and photographed under UV light.

3. Results and discussion

3.1. *Synthesis and characterization*

ITAP was prepared by the reaction of 5,6-diamino-1,10-phenanthroline with isatin in glacial acetic acid. The corresponding ruthenium(II) mixed-ligand complex was synthesized by the direct reaction of ITAP with the appropriate precursor complex in EtOH. The desired ruthenium(II) complex was isolated as the perchlorate and purified by column chromatography. In the ES-MS spectra for the Ru(II) complexes, all of the

expected signals $[M-ClO_4]^+$ and $[M-2ClO_4]^{2+}$ were observed. The measured molecular weights were consistent with expected values.

3.2. *Cyclic voltammetry*

The electrochemical behavior of $[Ru(dmb)_2(ITAP)]^{2+}$ has been examined in acetonitrile by cyclic voltammetry. As shown in figure 1, the Ru(II) complex exhibits well-defined waves corresponding to metal-based oxidation and successive ligand-based reduction in the sweep range from −2.0 to 2.0 V. This pattern is common to d^6 metal polypyridyl complexes, where the redox orbitals are localized on the individual ligands [29]. An oxidation wave corresponding to the Ru^{III}/Ru^{II} couple was observed at 1.21 V (*vs.* SCE), which is more negative than that of $[Ru(bpy)_3]^{2+}$ (1.28 V) [30]. The first reduction potential is usually controlled by the ligand having the most-stable lowest unoccupied molecular orbital (LUMO) [31]. Thus, the first reduction (−0.86 V) is assigned to ITAP. The two reversible reduction waves (−1.51 and −1.67 V) observed in the cyclic voltammogram, by comparing with $[Ru(bpy)_3]^{2+}$ and related Ru(II) polypyridyl complexes [32, 33], are assigned to dmb.

3.3. *Electronic absorption titration*

Electronic absorption spectra of $[Ru(dmb)_2(ITAP)]^{2+}$ consist of three resolved bands. The lowest energy band at 459 nm is assigned to the metal-to-ligand charge transfer (MLCT), the band at 356 nm is attributed to the $\pi \rightarrow \pi^*$ transition and the band at 285 nm is assigned to intraligand (IL) $\pi \rightarrow \pi^*$ transition by comparing with the spectra of other Ru(II) polypyridyl complexes [11, 32].

Figure 2 shows the electronic spectral traces of the Ru(II) complex titrated at room temperature with CT-DNA. With increasing concentration of CT-DNA, the hypochromism in the MLCT reaches as high as 22.2% and a red shift of 4 nm; the IL band displays hypochromism by about 34.3% and a red shift of 3 nm under the same experimental conditions. These spectral characteristics suggest that the complex

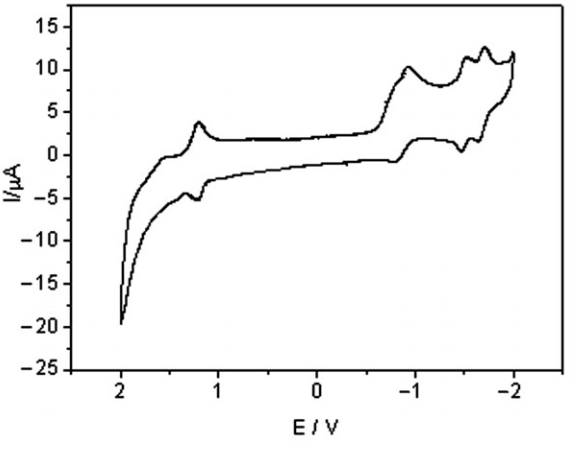

Figure 1. Cyclic voltammogram in MeCN.

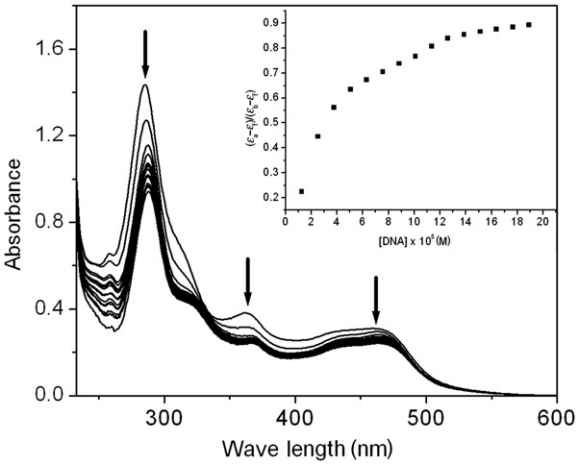

Figure 2. Absorption spectra of complex in Tris-HCl buffer in the presence of increasing amounts of DNA. [Ru] = 20 μM, [DNA] = 0–276 μM. The arrow shows the absorbance changes upon increase of DNA concentration. Plot of $(\varepsilon_a - \varepsilon_f)$ *vs.* DNA for the titration of DNA with Ru(II) complex.

interacts with DNA through a mode that involves stacking between the aromatic chromophore and the base pairs of DNA.

In order to further illustrate the binding strength of the complex, the intrinsic constant K_b was determined (inset in figure 2) by monitoring the changes of absorbance in the MLCT band with increasing the concentration of DNA; the intrinsic binding constant K_b is $(4.50 \pm 0.3) \times 10^4\,M^{-1}$ ($s = 1.65$), comparable with that of DNA-intercalative Ru(II) complexes (1.1×10^4–$4.8 \times 10^4\,M^{-1}$) [30, 34], but smaller than that observed for $[Ru(bpy)_2(dppz)]^{2+}$ ($>10^6$) and $[Ru(bpy)_2(ppd)]^{2+}$ (ppd = pteridino [7,6-f] [1, 10] phenanthroline-1,13(10H,12H)-dione, $K_b = (1.3 \pm 0.1) \times 10^6$) [11], due to the planarity of dppz and ppd being greater than ITAP. Absorption spectroscopic studies indicate that $[Ru(dmb)_2(ITAP)]^{2+}$ binds moderately to DNA by intercalation.

3.4. *Luminescence spectroscopic studies*

In Tris buffer solution at ambient temperature, $[Ru(dmb)_2(ITAP)]^{2+}$ emits luminescence with a maximum at 620 nm. Fixed amount (5 μM) of complex was titrated with increasing amounts of CT-DNA. The emission titration for complex with DNA is illustrated in figure 3. Upon addition of DNA, emission intensities increase steadily with increasing amounts of DNA until a stable emission intensity at [DNA]/[Ru] = 20 was observed; the emission intensity grows about 10.44 times larger than in the absence of DNA. This implies that complex strongly interacts with DNA and is protected by DNA efficiently, since the hydrophobic environment inside the DNA helix reduces the accessibility of solvent water to the complex and complex mobility is restricted at the binding site, leading to decrease in the vibrational modes of relaxation. The binding constant of the complex interacting with DNA is derived from emission spectra using the luminescence titration method. Binding data obtained from the emission spectra were fitted using the McGhee and Von Hippel equation [35] to acquire the binding parameters. The intrinsic binding constant K_b of $(7.8 \pm 0.2) \times 10^4$ ($n = 1.87$) was determined. Comparing with that

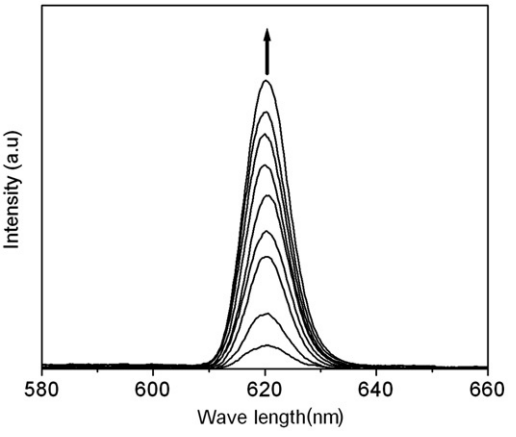

Figure 3. Emission spectra of complex in Tris-Cl buffer in the absence and presence of DNA. Arrow shows the intensity change upon increasing DNA concentration.

obtained from absorption spectra, the binding constant obtained from the McGhee–Von Hippel method are different from those obtained from the method suggested by Carter *et al*. [26]. This difference arises from the different spectroscopy and different calculation method. These binding constants reflect the great affinity between the complex and CT-DNA.

3.5. *Viscosity measurements*

To further explore the binding mode of $[Ru(dmb)_2(ITAP)]^{2+}$ with CT-DNA, viscosity measurements were carried out on CT-DNA by varying the concentration of added complex. The flow rates of DNA and Ru(II) complex-DNA through a capillary viscometer were measured. A classical intercalation model requires that the DNA helix is separated to accommodate the binding ligand, leading to an increase of DNA viscosity. In contrast, a partial, non-classical intercalation of ligand could bend (or kink) the DNA helix and reduce its effective length and, concomitantly, its viscosity [36, 37]. Under appropriate conditions, intercalation of drugs like EB causes a significant increase in the viscosity of DNA solutions due to increase in separation of base pairs at intercalation sites and, hence, an increase in overall contour length. Figure 4 shows the changes in viscosity upon addition of complex and EB. EB increases the relative specific viscosity for lengthening the DNA double helix through the intercalation mode. Upon increasing the amounts of $[Ru(dmb)_2(ITAP)]^{2+}$, the relative viscosity of CT-DNA solution increases steadily but is still smaller than those bound with EB. The results suggest that complex intercalates between the base pair of DNA.

3.6. *Thermal denaturation studies*

The melting of DNA is an important tool to study the interaction of transition metal complex with nucleic acid. Intercalation of small molecules into the double helix increases the helix melting temperature, the temperature at which the double helix denatures into single-stranded DNA, causing a hyperchromic effect on the absorption

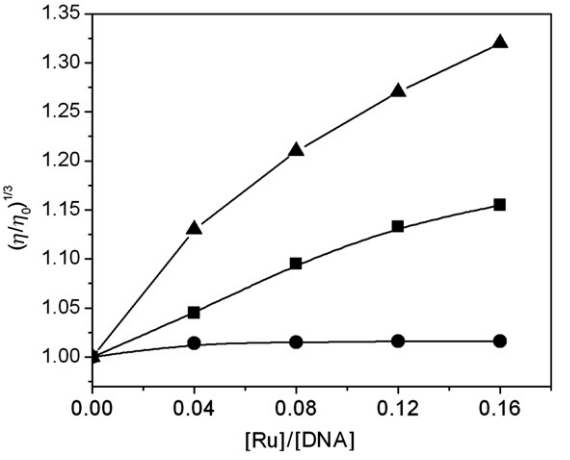

Figure 4. Effect of increasing amounts of EB (▲), $[Ru(dmb)_2(ITAP)]^{2+}$ (■), and $[Ru(bpy)_3]^{2+}$ (●) on the relative viscosity of CT-DNA at 28 (±0.1) C, [DNA] = 0.5 mM.

spectra of DNA bases ($\lambda_{max} = 260$ nm). Thus, the thermal behavior of DNA in the presence of complexes can give insight into their conformational changes. Thermal denaturation experiments carried out on DNA in the absence of complex revealed that T_m for the duplex is 75.2 ± 0.5°C under our experimental condition. As shown in figure 5, in the presence of the Ru(II) complex, the T_m of CT-DNA was successively increased. The observed change of melting temperatures (ΔT_m) in the presence of complex was 81.9 °C. The large increase in T_m ($\Delta T_m = 6.7$°C) is comparable to that observed for classical intercalators [8, 38–40]. The large change in T_m of CT-DNA in the presence of complex suggests an intercalative binding of the complex to DNA.

3.7. *Photo-induced cleavage of pBR322 DNA*

There is continuing interest in DNA endonucleolytic cleavage reactions activated by metal ions [41, 42]. Transition metal complexes of polypyridyl ligands are known to cleave DNA when irradiated by UV light [43]. When circular plasmid DNA is subjected to electrophoresis, relatively fast migration will be observed for the intact supercoil form (Form I). If scission occurs on one strand (nicking), the supercoil will relax to generate a slower-moving open circular form (Form II) [44]. The cleavage reaction on plasmid DNA in the presence of $[Ru(dmb)_2(ITAP)]^{2+}$ can be monitored by agarose gel electrophoresis. Supplementary material shows the gel electrophoresis separation of pBR322 DNA after incubation with the Ru(II) complex and irradiation at 365 nm for 1 h. No DNA cleavage was observed for control in which complex was absent, or incubation of the plasmid DNA with the Ru(II) complex in dark (data not presented). By increasing the concentration of the Ru(II) complex, the amount of Form I of pBR 322 DNA diminishes gradually, whereas Form II increases.

One of the most interesting electrophoretic results of $[Ru(dmb)_2(ITAP)]^{2+}$ takes place when the DNA cleavage experiment has been carried out in the presence of D-mannitol, dimethylsulfoxide (DMSO), superoxide dismutase (SOD) enzyme, and histidine in order to observe the reactive species that are responsible for the photoactivated cleavage

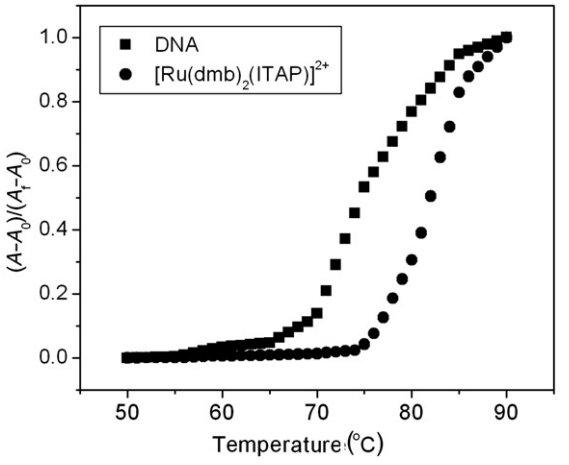

Figure 5. Melting temperature curves of DNA in the absence (■) and presence of complex (●). [Ru] = 20 μM, [DNA] = 80 μM.

of the plasmid DNA (Supplementary Material). The DNA cleavage of the plasmid by complex was not inhibited in the presence of hydroxyl radical (OH•) scavengers such as mannitol [45] and DMSO [46], indicating that hydroxyl radical was not likely to be the cleaving agent. In the presence of SOD, a facile superoxide anion radical ($O_2^{\bullet -}$) quencher, the cleavage was obviously improved, which indicated that $O_2^{\bullet -}$ might be an inhibitor in the photoactivated cleavage of the plasmid and reducing the amount of $O_2^{\bullet -}$ can improve the cleavage effect. SOD strongly enhancing the yield of cleavage has also been observed in photoactivated cleavage using $[Ru(bpz)_3]^{2+}$ (bpz is 2,2′-bipyrazyl) with synthetic oligonucleotides [47]. The DNA cleavage was inhibited in the presence of the singlet oxygen ($^1O_2$) scavenger histidine [48], suggesting that $^1O_2$ is likely to be the reactive species responsible for cleavage. Similar cases have been observed in the DNA photocleavage by $[Ru(phen)_3]^{2+}$, which is attributed to an $^1O_2$-based mechanism [49].

4. Conclusion

ITAP and its complex $[Ru(dmb)_2(ITAP)]^{2+}$ were synthesized and characterized by elemental analysis, FAB-MS, ESI-MS, and ^1H NMR. The DNA-binding properties have been studied by electronic absorption titration, thermal denaturation, viscosity measurements, and photo-induced cleavage. The viscosity measurements and thermal denaturation show that the complex interacts with CT-DNA by intercalative mode. Mechanistic studies of photocleavage reveal that singlet oxygen ($^1O_2$) and superoxide anion radical ($O_2^{\bullet -}$) may play a role in the photocleavage.

Acknowledgements

We are grateful to the Science and Technology Foundation of Guangdong Province (No. 2004B33301029) and Guangdong Pharmaceutical University for financial support.

References

[1] C.J. Burrows, S.E. Rokita. *Acc. Chem. Res.*, **27**, 295 (1994).
[2] A.M. Pyle, J.K. Barton. In *Progress in Inorganic Chemistry*, S.J. Lippard (Ed.), Vol. 38, p. 413, Wiley, New York (1990).
[3] T.D. Tullius. *Metal–DNA Chemistry, ACS Symposium Series*, Vol. 402, American Chemical Society, Washington, DC (1989).
[4] A.R. Banerjee, J.A. Jaeger, D.H. Turner. *Biochemistry*, **32**, 153 (1993).
[5] A.E. Friedman, C.V. Kumar, N.J. Turro, J.K. Barton. *Nucleic Acids Res.*, **19**, 2595 (1991).
[6] J.C. Chambron, J.P. Sauvage, E. Amouyal, P. Koffi. *New J. Chem.*, **9**, 527 (1985).
[7] Y. Jenkins, A.E. Friedman, N.J. Turro, J.K. Barton. *Biochemistry*, **31**, 10809 (1992).
[8] A.E. Friedman, J.C. Chambron, J.P. Sauvage, N.J. Turro, J.K. Barton. *J. Am. Chem. Soc.*, **112**, 4960 (1990).
[9] P.B. Dervan. *Science*, **232**, 464 (1986).
[10] C.H. Zimmer, U. Wahnert. *Prog. Biophys. Mol. Biol.*, **47**, 31 (1986).
[11] F. Gao, H. Chao, F. Zhou, Y.X. Yuan, B. Peng, L.N. Ji. *J. Inorg. Biochem.*, **100**, 1487 (2006).
[12] Y.J. Liu, W.J. Mei, J.Z. Lu, H.J. Zhao, L.X. He, F.H. Wu. *J. Coord. Chem.*, **61**(20), 3213 (2008).
[13] Y.J. Liu, H. Chao, Y.X. Yuan, H.J. Yu, L.N. Ji. *Inorg. Chim. Acta*, **359**, 3807 (2006).
[14] L.F. Tan, F. Wang, H. Chao, Y.F. Zhou, C. Wen. *J. Inorg. Biochem.*, **101**(4), 700 (2007).
[15] W.J. Mei, J. Liu, H. Chao, L.N. Ji. *Transition Met. Chem.*, **28**, 852 (2003).
[16] D. Magda, M. Wright, R.A. Miller, J.L. Sessler, P.I. Sansom. *J. Am. Chem. Soc.*, **117**, 3629 (1995).
[17] S. Swavey, K.J. Brewer. *Inorg. Chem.*, **41**, 6196 (2002).
[18] A.E. Friedman, J.C. Chambron, J.P. Sauvage, N.J. Turro, J.K. Barton. *J. Am. Chem. Soc.*, **112**, 4960 (1990).
[19] J. Marmur. *J. Mol. Biol.*, **3**, 208 (1961).
[20] M.F. Reichmann, S.A. Rice, C.A. Thomas, P. Doty. *J. Am. Chem. Soc.*, **76**, 3047 (1954).
[21] G.F. Smith, F.W. Cogle. *J. Org. Chem.*, **65**, 452 (1943).
[22] J. Bolger, A. Gourdon, E. Ishow, J.P. Launay. *Inorg. Chem.*, **35**(10), 2937 (1996).
[23] B.P. Sullivan, D.J. Salmon, T.J. Meyer. *Inorg. Chem.*, **17**, 3334 (1978).
[24] J.K. Barton, J.J. Dannenberg, A.L. Raphael. *J. Am. Chem. Soc.*, **106**, 2172 (1984).
[25] S.R. Smith, G.A. Neyhart, W.A. Karlsbeck, H.H. Thorp. *New J. Chem.*, **18**, 397 (1994).
[26] M.T. Carter, M. Rodriguez, A.J. Bard. *J. Am. Chem. Soc.*, **111**, 8901 (1989).
[27] J.B. Chaires, N. Dattagupta, D.M. Crothers. *Biochemistry*, **21**, 3933 (1982).
[28] G. Cohen, H. Eisenberg. *Biopolymers*, **8**, 45 (1969).
[29] B.K. Ghosh, A. Chakra-Vorty. *Coord. Chem. Rev.*, **95**, 239 (1989).
[30] T. Matsumura-Inoue. *J. Electroanal. Chem.*, **95**, 109 (1979).
[31] J.E.B. Johnson, R.R. Ruminski. *Inorg. Chim. Acta*, **208**, 231 (1993).
[32] Y.J. Liu, X.Y. Wei, F.H. Wu, W.J. Mei, L.X. He. *Spectrochim. Acta, Part A*, **70**, 171 (2008).
[33] L.F. Tan, H. Chao. *Inorg. Chim. Acta*, **360**, 2016 (2007).
[34] A.M. Pyle, J.P. Rehmann, R. Meshoyrer, C.V. Kumar, N.J. Turro, J.K. Barton. *J. Am. Chem. Soc.*, **111**, 3051 (1989).
[35] J.D. McGhee, P.H. Von Hippel. *J. Mol. Biol.*, **86**, 469 (1974).
[36] S. Satyanarayana, J.C. Dabroniak, J.B. Chaires. *Biochemistry*, **31**, 9319 (1992).
[37] S. Satyanaryana, J.C. Daborusak, J.B. Chaires. *Biochemistry*, **32**, 2573 (1993).
[38] D.L. Boger, B.E. Fenk, S.R. Brunette, W.C. Tse, M.P. Hedrick. *J. Am. Chem. Soc.*, **123**, 5878 (2001).
[39] C.M. Dupureur, J.K. Barton. *Inorg. Chem.*, **36**, 33 (1997).
[40] C.V. Kumar, E.H. Asuncion. *J. Am. Chem. Soc.*, **115**, 8547 (1993).
[41] D.S. Sigman. *Acc. Chem. Res.*, **19**, 180 (1986).
[42] B. Armitage. *Chem. Rev.*, **98**, 1171 (1998).
[43] J.K. Barton, A.L. Raphael. *J. Am. Chem. Soc.*, **106**, 2466 (1984).
[44] H.Y. Mei, J.K. Barton. *Proc. Natl. Acad. Sci. USA*, **85**, 1339 (1988).
[45] C.C. Cheng, S.E. Rokita, C.J. Burrows. *Angew. Chem. Int. Ed. Engl.*, **32**, 277 (1993).
[46] S.A. Lesko, R.J. Lorentzen, P.O. Ts'o. *Biochemistry*, **19**, 3023 (1980).
[47] L. Bijeire, B. Elias, J.P. Souchard, E. Gicquel, C. Moucheron, A. Kirsch-De Mesmaeker, P. Vicendo. *Biochemistry*, **45**, 6160 (2006).
[48] R. Nilsson, P.B. Merkel, D.R. Kearns. *Photochem. Photobiol.*, **16**, 117 (1972).
[49] H.Y. Mei, J.K. Barton. *Proc. Natl. Acad. Sci. USA*, **85**, 1339 (1988).